Available online at www.sciencedirect.com
ScienceDirect
Earth and Planetary Science Letters 249 (2006) 326–336
EPSL
www.elsevier.com/locate/epsl

Pleistocene glacial terminations triggered by synchronous changes in Southern and Northern Hemisphere insolation: The insolation canon hypothesis

K.G. Schulz [a,*], R.E. Zeebe [b]

[a] Leibniz Institute for Marine Sciences, Düsternbrooker Weg 20, 24105 Kiel, Germany
[b] University of Hawaii at Manoa SOEST Department of Oceanography 1000 Pope Road, MSB 504 Honolulu, HI 96822, USA

Received 16 August 2005; received in revised form 4 May 2006; accepted 7 July 2006
Available online 21 August 2006
Editor: H. Elderfield

Abstract

Throughout the last ~ 900 kyr, the Late Pleistocene, Earth has experienced periods of cold glacial climate, punctuated by seven abrupt transitions to warm interglacials, the so-called terminations. Although most of glacial ice is located in the Northern Hemisphere (NH), the Southern Hemisphere (SH) seems to play a crucial role in deglaciation. Variation in the seasonal distribution of solar insolation is one candidate for the cause of these climatic shifts. But so far, no simple mechanism has been identified. Here we present a mathematical analysis of variations in midsummer insolation in both hemispheres at 65° latitude. Applying this analysis to the entire Pleistocene, the last 2 Myr, we find that prior to each termination the insolation in both hemispheres increases in concert, with a SH lead. Introducing time and energy thresholds to these overlaps, calculated times for the onsets of the seven terminations by this insolation canon (exceptional overlaps meeting the two threshold prerequisites) are ~ 23, 139, 253, 345, 419, 546 and 632 kyr BP, perfectly matching the geologic record. The timing originates from the interplay between the two orbital parameters obliquity and precession, explaining why terminations occur at integer multiple of the precessional cycle. There is no such constellation between 1 and 2 Myr BP, the Early Pleistocene, in agreement with Earth's climate at that time. This change in orbital forcing coincides with the Mid Pleistocene Revolution, separating the Late from the Early Pleistocene. Therefore, we hypothesize that the insolation canon is the trigger for glacial terminations.

Keywords: glacial terminations; insolation; Northern Hemisphere; Southern Hemisphere

1. Introduction

Earth has gone through large climatic shifts during the past ~ 900 kyr, the Late Pleistocene, with seven major glaciations [1,2] (see Fig. 1A). These glaciations were punctuated by seven mostly rapid transitions to warm interglacial climate conditions, occurring approximately every 100 kyr (Fig. 1B). This feature is absent in climate records from the Early Pleistocene (1.1–2 Myr), which are dominated by a 41 kyr periodicity (Fig. 1C), marking the Mid Pleistocene Revolution (MPR). The so-called 100 kyr glacial/interglacial cycles are associated with the built-up and melting of enormous Northern Hemisphere (NH) ice sheets extending over Canada and Scandinavia. Therefore, it has been suggested that changes in NH

* Corresponding author. Tel.: +49 431 600 4510; fax: +49 431 600 1515.
E-mail address: kschulz@ifm-geomar.de (K.G. Schulz).

0012-821X/$ - see front matter © 2006 Elsevier B.V. All rights reserved.
doi:10.1016/j.epsl.2006.07.004

summer insolation are driving these climatic shifts [3]. However, only recently it became apparent that also the ice sheet in the Southern Hemisphere (SH) is reacting to glacial terminations [4] and that the Antarctic might play a pivotal role in these climatic events [5,6]. Additionally, considering changes in NH insolation as the sole driver poses several paradoxes. The astronomical theory of long-term changes in orbital parameters [3,7–9] predicts quasi-periodic variations of eccentricity, obliquity and precession of the equinoxes with dominant frequencies centered around 100, 41 and 23/19 kyr, respectively. While the 19/23 and 41 kyr cycles have been demonstrated to be coherent with the amplitude of insolation forcing in numerous climate records [10], the quasi 100 kyr glacial/interglacial cycle remains a mystery, since the amplitude of the eccentricity forcing is much too small to drive this cycle. Furthermore, the eccentricity forcing is partly out of phase [10]. Besides this '100 kyr problem' (for a review see [11,12]), explanation for the 'stage 11 problem' (the most prominent termination occurs at times of comparatively low orbital variations) and the 'Late Pleistocene transition problem' (the miraculous shift of climate cyclicity at the MPR) are still lacking [13]. Given the apparent involvement of both hemispheres in glacial terminations, a mechanism triggering this global phenomenon should therefore not only provide answers to the paradoxes outlined above but also encompass and connect both hemispheres.

2. Methods

2.1. The insolation analysis

We examined changes in midsummer insolation at 65 ° North (June 21) together with corresponding changes

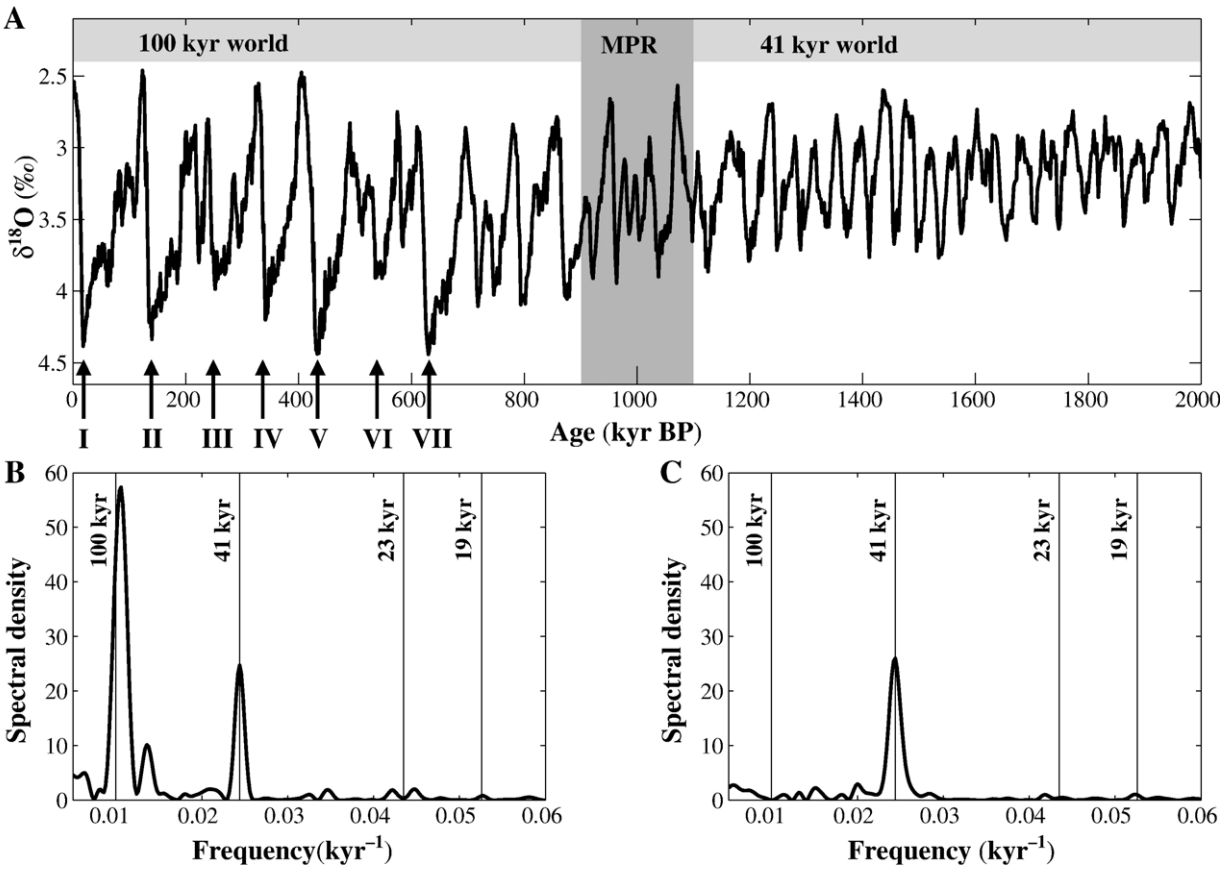

Fig. 1. Comparison of climate variability in the Late Pleistocene (100 kyr world) and the Early Pleistocene (41 kyr world). (A) $\delta^{18}O$ of the LR04 benthic stack [33] against time over the entire Pleistocene. The Mid Pleistocene Revolution (MPR) marks the shift from the 41 kyr to the 100 kyr world. The seven glacial terminations of the Late Pleistocene are shown in Roman numbers. (B) Power spectral densities of the above $\delta^{18}O$ signal (detrended and normalized) against their frequencies during the last 900 kyr, the Late Pleistocene, and (C) between 1100 to 2000 kyr BP, the Early Pleistocene.

in the South (December 21) of the last 2 Myr. The analysis was performed on the (1,1) astronomical solution for Earth's orbital parameters given in [9] with a solar constant set to 1368 Wm^{-2} at a step size of 100 yr (provided by J. Laskar). This astronomical solution incorporates present day values for dynamical ellipticity and tidal dissipation (1,1). Changes in tidal dissipation, resulting from the stresses exerted on Earth by the Moon and the Sun, and dynamical ellipticity, associated with mass load redistribution, e.g. during ice-age cycles, influence the phasing of precession and obliquity [14]. However, it is reasonable to use present day values and to keep them constant, as they remained close to today's values during the last millions of years [15,16].

3. Results and discussion

3.1. The overlaps

We found that prior to each termination as identified by the geologic record the insolation in both hemispheres is increasing simultaneously and that the SH increase leads the NH, a feature we refer to as 'overlap' hereafter. These events are not exclusively restricted to the occurrence of terminations. There is a total number of 22 between 2 and 1 Myr BP (Fig. 2A) and about the same (23) between 1 Myr and present day (Fig. 2B). However, the mean length of these synchronous midsummer insolation increases is on average about 40% longer in the Late Pleistocene (~ 1300 yr) compared to the Early Pleistocene (~ 800 yr). Moreover, at all terminations the length of an overlap is always equal to or longer than 1000 yr. Comparison of the Late and the Early Pleistocene shows that while there are 13 of these prolonged (equal to or longer than 1000 yr) overlaps between 1 Myr and present day (Fig. 2A) there are only 6 between 2 and 1 Myr BP (Fig. 2B). Furthermore, the energy supplied during the increase of Southern and Northern Hemisphere midsummer insolation at the prolonged overlaps in the Late Pleistocene is on average about 15% higher and about 20% higher at glacial terminations, compared to those in the Early Pleistocene.

We thoroughly checked whether the overlaps, the synchronous increase in SH and NH insolation with a

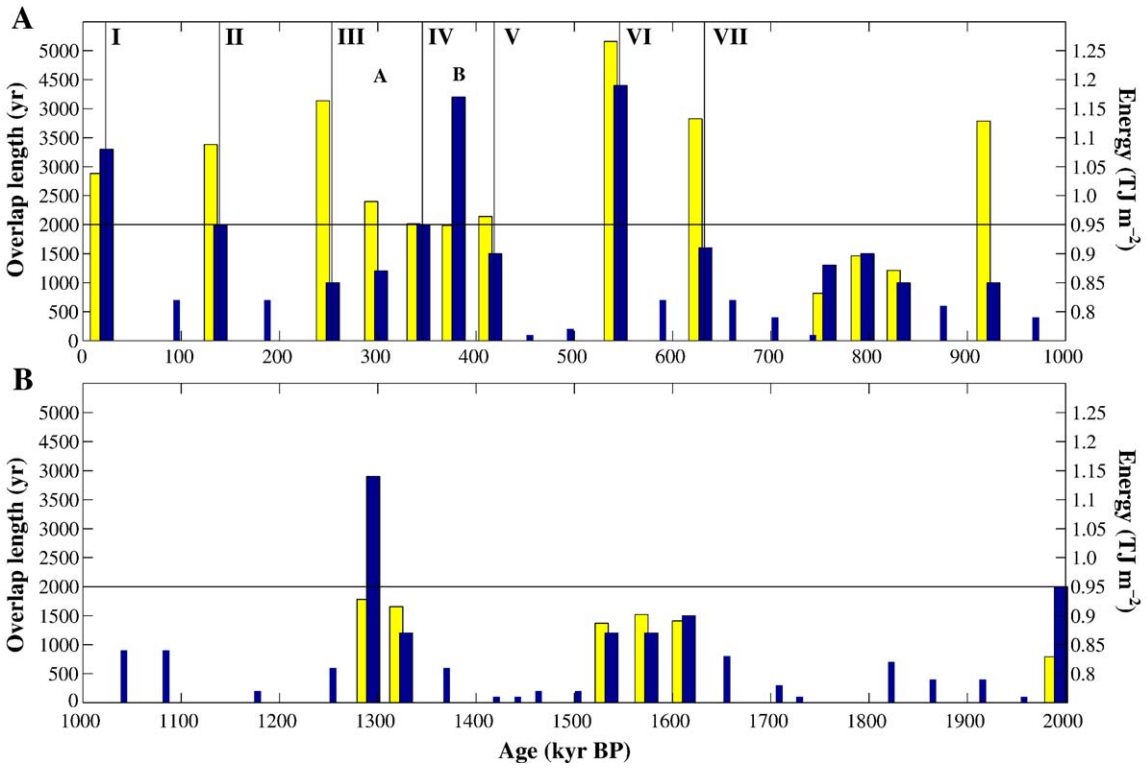

Fig. 2. All overlaps of the last 2 Myr and corresponding energy (energy only shown if overlap is equal to or longer than 1000 yr). Blue bars in (A) (0–1 Myr BP) and (B) (1–2 Myr BP) indicate the length of an overlap (thin bars < 1000 yr, thick bars ≥ 1000 yr), yellow bars the total energy supplied (see Fig. 3 and caption to Fig. 3 for details). The black horizontal line represents our energy constraint, see text for details. Roman numbers indicate terminations. 'A' and 'B' refer to Event A and B, respectively (see text for details).

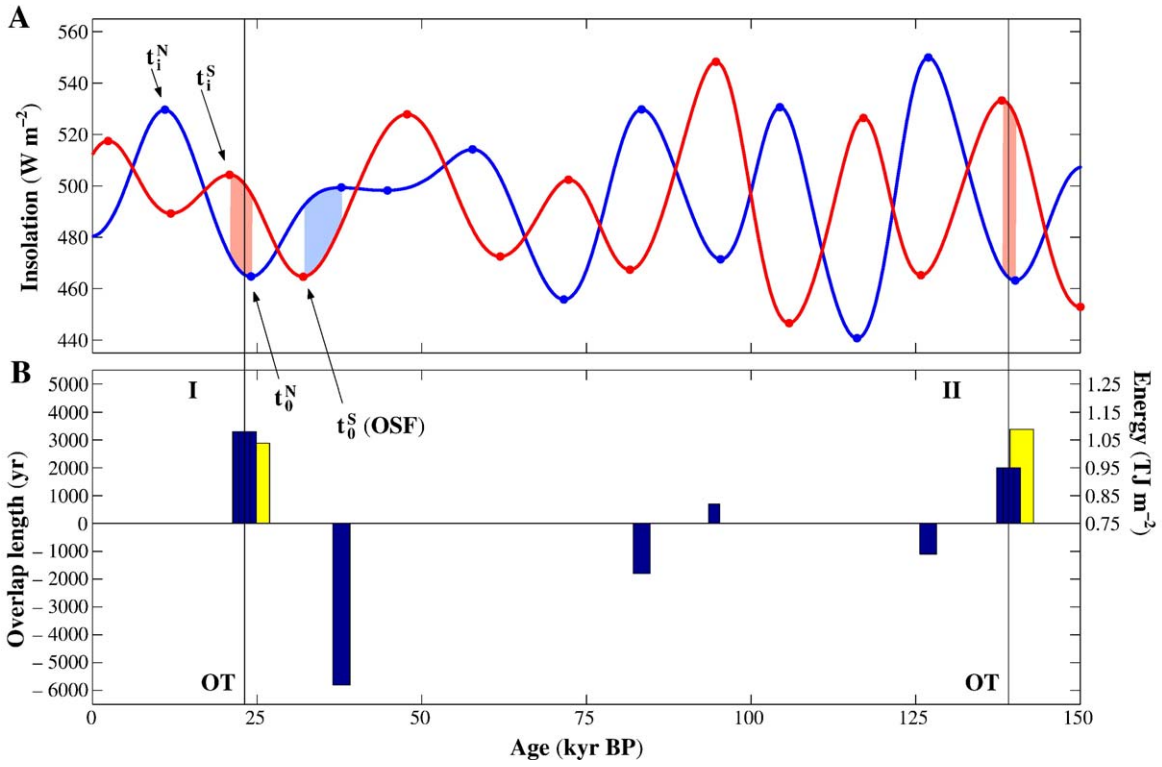

Fig. 3. Graphical illustration of the mathematical analysis used to identify terminations (shown in Roman numbers). (A) Northern midsummer insolation at 65 °N (blue), its extrema (circles), and southern midsummer insolation at 65 °S (red) and its extrema (circles) against time. t_0^S and t_0^N are the times for the onset of SH and NH insolation increase and t_i^S and t_i^N are their following maxima, respectively. t_0^S is defined as the Onset of Southern Hemisphere Forcing (OSF) and 1000 yr after t_0^N, the Onset of Termination (OT) is triggered, as marked by vertical lines. Shaded red areas illustrate the overlaps during SH and NH insolation increase, the insolation canon. Note that a prerequisite for this overlap is that the SH precedes the NH midsummer insolation increase. The shaded blue area highlights the time overlap during SH and NH insolation decrease, with a SH lead ('negative' insolation canon) prior to termination I (see text for details). (B) Thick blue bars represent the length of an overlap which meets our two termination conditions. Yellow bars denote the total energy supplied during the corresponding increase of southern and northern midsummer insolation (I_S and I_N, respectively), i.e. $E = \int_{t_0^S}^{t_i^S} I_S(t)\mathrm{d}t + \int_{t_0^N}^{t_i^N} I_N(t)\mathrm{d}t$. Thin blue bars represent overlaps shorter than 1000 yr (pos. ordinate) and overlaps of the 'negative' insolation canon (neg. ordinate).

SH lead, determined with this astronomical solution depends on the solution employed for Earth's orbital elements. Using the solution given in [7] for the last 800 kyr and the solution given in [8] for the time between 0.8 and 2 Myr BP, we obtained essentially the same results. Thus, the overlaps are a robust feature of different solutions for Earth's orbital parameters.

3.2. The insolation canon

There is no significant difference in the total number of overlaps between 2–1 and 1–0 Myr. However, at Late Pleistocene glacial terminations the overlaps are exceptional because they are longer and supply more energy than others. This leads us to postulate two prerequisites for a glacial termination. First, and most importantly, the overlap has to be equal to or longer than 1000 yr. Second, total energy supplied during the increase of southern and northern midsummer insolation has to exceed a threshold of 0.95 TJ m^{-2}, which is the lowest observed at a termination. These thresholds between the two extreme states of glacial and interglacial climate (here, time and energy) can be considered the simplest representation for Earth's nonlinear climate system [17,18].

In the following the chronology of events around a glacial termination is described, as detected by our analysis (see Fig. 3A). 1) The SH midsummer insolation reaches a minimum (t_0^S) and starts to increase, defined here as Onset of SH Forcing (OSF). 2) While the SH insolation is still increasing, the NH insolation reaches a minimum (t_0^N) and also starts to rise. 3) After 1000 yr of simultaneous increase the onset of a termination (OT) is triggered. Shortly after this event, SH insolation reaches a maximum and starts to decrease. 4) NH insolation continues to increase until

reaching a maximum 10–15 kyr later. During this increase of midsummer insolation in both hemispheres the total energy supplied always exceeds the threshold of 0.95 TJ m^{-2}. In analogy to its counterpart in music we refer to this constellation as the 'insolation canon' (exceptional overlap meeting the two prerequisites).

The resulting OTs perfectly match the geologic record (Fig. 4A), coinciding with marine $\delta^{18}O$ maxima, which to a first approximation reflect maxima in ice sheet extension [19]. Additionally, the OTs which we date 23.1, 139.1, 253.3, 345.4, 418.6, 546.2 and 632.3 kyr BP roughly occur 10 kyr prior to the corresponding midpoint of termination, as suggested by various marine $\delta^{18}O$ records (Table 1). An exception is termination V, where OT and the midpoint of termination are indistinguishably close. Moreover, the time intervals between our onsets of terminations of 86, 128, 73, 92, 114, 116 kyr (terminations VII–VI, VI–V, V–IV, IV–III, III–II, II–I, respectively) agree very well with intervals between midpoints of terminations in marine $\delta^{18}O$ records, independent of the dating method applied (Table 1).

In addition to the sound prediction of the timing of glacial terminations there are three more interesting results. First, there are two times at which only shortly after a termination an overlap longer than 1000 yr occurs. Event A lies between termination IV and III at 302.4 kyr and Event B between termination V and IV at 381.3 kyr BP (Fig. 2A). As those events occur only 40 kyr after a termination, Earth's climate was not in full glacial mode and hence seems not to have responded to this trigger. Second, there is not a single termination trigger between 2 and 1 Myr (Fig. 2B). Third, our analysis reveals one 'additional' termination trigger at 925.6 kyr BP, roughly coinciding with the Mid Pleistocene revolution (MPR), the switch from a 41 kyr to a 100 kyr dominated climate signal [20].

3.3. Origin of overlaps

The question arises, how the overlaps identified above are generated and what is determining their

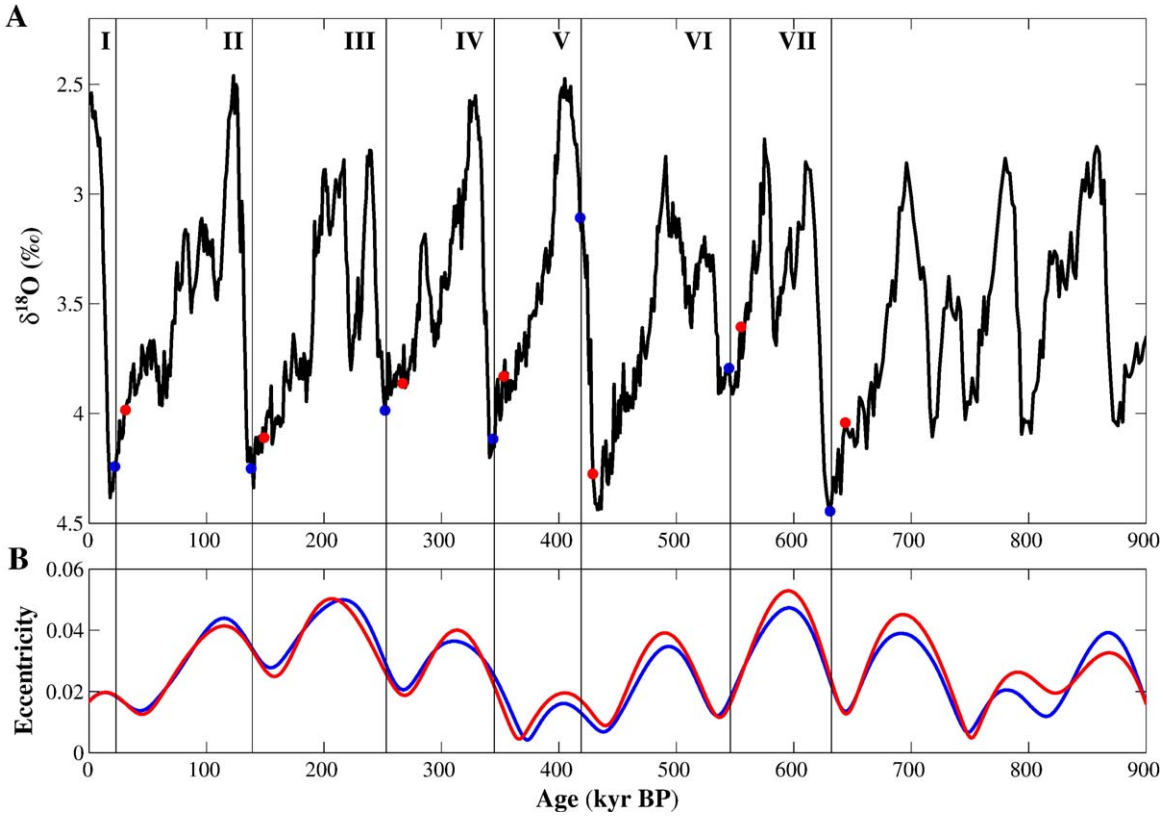

Fig. 4. Comparison of the stacked $\delta^{18}O$ LR04 record [33], terminations and eccentricity forcing. (A) $\delta^{18}O$ of this benthic stack against time (black line). Roman numbers indicate terminations. Blue circles and vertical lines represent the times of the Onset of Termination (OT), as determined in this study (see text for details). Red circles denote the Onset of Southern Hemisphere Forcing (OSF) before a termination, i.e. the start of increasing midsummer insolation at 65 °S. See also Table 1 for a detailed comparison of OT with terminations determined in various marine $\delta^{18}O$ records. (B) Eccentricity variations according to the astronomical solution of [7] (red) and [9] (blue) against time.

Table 1
Comparison between results from this study and various deep-sea records[a]

Termination (kyr BP)								
Author	I	II	III	IV	V	VI	VII	Method
This work, OT	23.1	139.1	253.3	345.4	418.6	546.2	632.3	1
RAYMO			247.9	339.3	423.6	534.5	621.6	2
L & R	14	130	243	337	424	533	621	3
H & W	11	129	239	332	419	532	623	4
SPECMAP	11	128	244	337	423	531	621	5
Δt_{OT-MT} (kyr)								
	11.1	10.1	9.8	9.0		13.6	10.7	
Δt_{Term} (kyr)								
This work		116	114	92	73	128	86	
RAYMO				91	84	111	87	
L & R		116	113	91	87	109	88	
H & W		118	110	93	87	113	91	
SPECMAP		117	116	93	86	108	90	

[a]OT refers to the Onset of Termination obtained in our analysis in kyr BP. For comparison the midpoints of termination (kyr BP) determined by Raymo [22] (RAYMO), Lisiecki and Raymo [33] (L & R), Huybers and Wunsch [23] (H & W) and Imbrie et al. [34] (SPECMAP) are shown. Additionally, the offset in kyr between our calculated OTs and the mean of the midpoints of termination (MT) are tabulated (Δt_{OT-MT}). Δt_{Term} values denote the time interval between two terminations in kyr. Methods applied are: mathematical analysis, this work (1), depth-derived with constant accumulation rate assumed (2), automated graphic correlation algorithm (3), depth-derived with sedimentation model (4), orbitally tuned (5).

duration. In order to separate the individual influence of each of the orbital parameters precession of the equinoxes, obliquity and eccentricity, we analyzed artificial insolation curves generated by a truncated Fourier series of the form

$$I(t) = \sum_{k=1}^{4} a_k \sin(\omega_k * t) \quad (1)$$

with $I(t)$ being the insolation at time t, $\omega_k = 2\pi / T_k$, and T_k being the oscillation periods of 100 kyr, 41 kyr, 23 kyr and 19 kyr, representing those of eccentricity, obliquity and precession of the equinoxes, respectively. The Fourier-coefficients a_k were set to 0.1, 0.7, 1, 1 for Northern Hemisphere insolation and to 0.1, 0.7, −1, −1 for Southern Hemisphere insolation, representing the amplitude in the respective frequency bands. These two insolation curves exhibit a very similar density spectrum to that of insolation during the last 2 Myr as given by the solution in [9], i.e. dominant frequencies around 41, 23 and 19 kyr (compare Fig. 5). But most importantly, the artificial insolation curves also generate about 21 overlaps per million years. Setting the 100 kyr amplitude to zero (no eccentricity) hardly affects the number and average duration of an overlap. However, setting either the 41 kyr (no obliquity) or the 23 and 19 kyr (no precession) amplitude to zero, there are no overlaps because insolation changes are completely anti-phased or in-phase, respectively. In general, the ratio of the spectral densities of obliquity (41 kyr) and precession of the equinoxes (23, 19 kyr) determine the length of an overlap as this shifts the NH insolation minima relative to SH insolation maxima between the two extremes of completely anti-phased and completely in-phase. As demonstrated above it is possible to separate the influence of each orbital parameter on the overlaps by using artificial insolation curves. Naturally, however, eccentricity combines with the precession of Earth's axis of rotation and modulates the precession of the equinoxes (see Eq. (1) in [14]). This combination is the reason for the change in spectral power densities, especially in the 19 kyr frequency band in the Early compared to the Late Pleistocene (Fig. 5B and C) and explains why the number of prolonged overlaps (equal or longer 1000 yr) significantly increases around 1 Myr BP. Thus, we have identified a change in orbital forcing around the MPR.

In summary, we hypothesize that the glacial termination trigger is the synchronous, prolonged (≥1000 yr) increase in SH and NH insolation, the insolation canon. It stems from an interplay between the three orbital parameters precession, obliquity and eccentricity. The timing of all overlaps is generated by a modulation of insolation through variations in obliquity and precession. This readily explains why the time interval between two consecutive terminations is always an integer multiple of the precessional cycles in this interval [21]. The duration of an overlap, however, is modulated also by eccentricity. Most importantly, the insolation canon explains why the

number of precessional cycles between two terminations is not fixed (for example every fourth or fifth).

3.4. The three classical problems

Although the concept of the insolation canon provides a possible solution for the '100 kyr problem', one of the three classical problems of Pleistocene research [13], several questions remain regarding the other two problems ('Late Pleistocene transition' and 'stage 11').

The Late Pleistocene transition problem: While our analysis provides the trigger for glacial terminations, the trigger involved in the initiation of a glaciation itself remains unclear. However, besides the finding that orbital forcing changed in the Pleistocene about 1 Myr BP at the MPR (i.e. the absence of the insolation canon in the Early and its occurrence in the Late Pleistocene), our analysis furthermore identifies two extra clues for the beginning of the 100 kyr glaciations after the MPR. 1) The first occurrence of the insolation canon is dated at 926 kyr BP. This may have shifted Earth's climate system to a different mode of operation, leading to the initiation of 100 kyr ice sheets. 2) A 'negative' forcing, analogous to the 'positive' forcing (Fig. 2B), could be involved, i.e. synchronous midsummer insolation decrease in both hemispheres with a SH lead. In the last 2 Myr this opposing 'negative' forcing exhibits a similar distribution and energy pattern as the 'positive' termination forcing (Fig. 6). Applying analogous energy and time thresholds, there is only one of these events prior to the MPR compared to eight afterwards. Interestingly, the first occurrence of such 'negative' insolation canon in the Late Pleistocene is 650 kyr BP, only about 20 kyr before termination VII. In this short period of time, marine $\delta^{18}O$ reached a hitherto unprecedented high value (compare Fig. 1A and Fig. 4A).

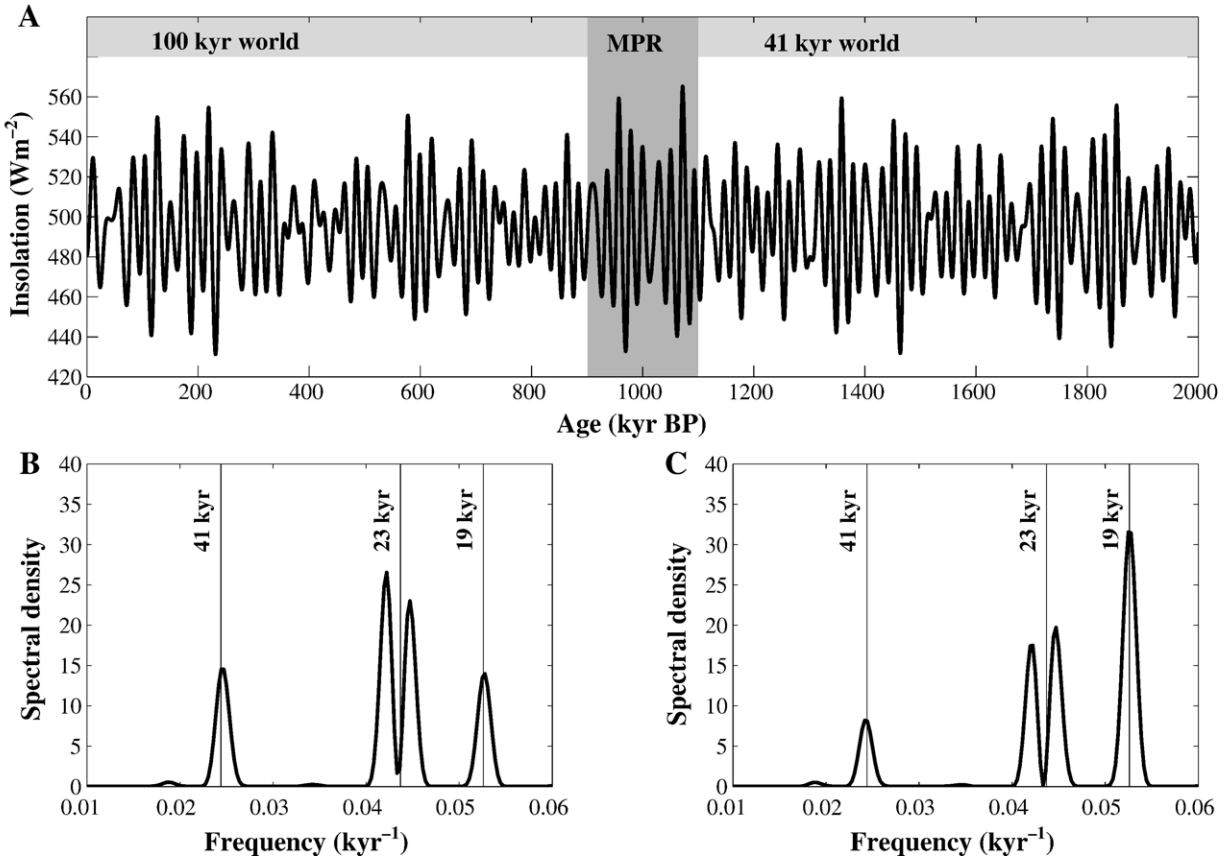

Fig. 5. Comparison of variability in insolation between the Late and Early Pleistocene. (A) Midsummer insolation at 65 °N of the last 2 Myr. (B) Power spectral densities of the above insolation curve (detrended and normalized) against their frequencies during the last 900 kyr, the Late Pleistocene, and (C) between 1100 and 2000 kyr BP, the Early Pleistocene. Note that spectral analysis of the variability in insolation at 65 °S gives the same results.

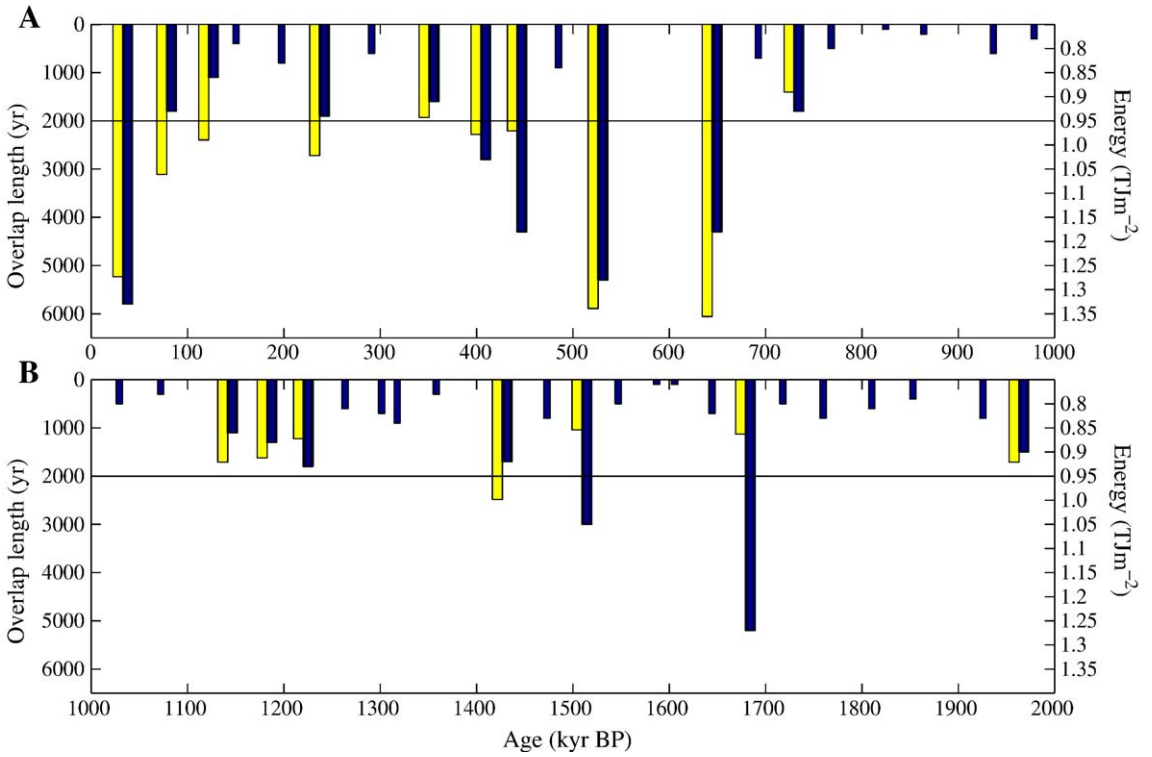

Fig. 6. The 'negative' insolation canon with its overlaps of the last 2 Myr and corresponding energy (energy only shown if overlap is equal to or longer than 1000 yr). In analogy to the 'positive' insolation canon (see caption to Fig. 3 for details), total energy during insolation decrease was calculated as the integrated area between insolation curves and twice the value of the average insolation during the last 2 Myr. This seemingly arbitrary baseline was chosen to ensure comparability with energy values of the 'positive' insolation canon. The resulting energy can be pictured as a mirror image of the energy increase and is representative for the total energy decrease of the 'negative' insolation canon. Blue bars in (A) (0–1 Myr BP) and (B) (1–2 Myr BP) indicate the length of an overlap (thin bars <1000 yr, thick bars ≥ 1000 yr), yellow bars represent a measure for the total energy decrease. The black horizontal line illustrates our energy constraint.

Additionally, considering the insolation canon (prolonged overlap providing a critical amount of energy) as an exceptional case within all overlaps, could explain the shift from a 41 kyr to a 100 kyr periodicity in global ice volume at the MPR. While in both, the Early and the Late Pleistocene, power spectral densities in marine δ^{18}O are about the same around the 41 kyr frequency band, the Late Pleistocene is characterized by the occurrence of an additional 100 kyr cyclicity (Fig. 1B, C). Constructing a sawtooth motive from the occurrence of all overlaps (Fig. 7A) reveals that the dominant frequency in this oscillator is around 41 kyr (Fig. 7B and C), both in the Early and Late Pleistocene. Constructing a sawtooth motive only from the occurrence of the insolation canon during the Late Pleistocene (omitting event A and B at which Earth's climate did not respond to the insolation canon) shows that this oscillator is dominated by a 100 kyr cyclicity (Fig. 7B). Combination of both forcings could explain the appearance of a 100 kyr cyclicity in global climate variability during the Late Pleistocene while the 41 kyr cyclicity remains unchanged throughout the entire Pleistocene (Fig. 7B and C). However, it is emphasized that 'cyclicity' as suggested by the spectral analysis should be regarded as a 'pseudo-cyclicity'. Both, the ice volume variability in the Early and Late Pleistocene do not follow a regular 41 kyr or 100 kyr periodicity and the occurrence of terminations appears to be quantized rather than regularly spaced (see [21] and Table 1). Finally, the concept of overlaps could also readily explain why marine δ^{18}O records do not show a strong precessional signal (around 23 and 19 kyr) like insolation itself (compare Figs. 1 and 5).

The stage 11 problem: At first glance the problem that the most prominent termination occurs at times of comparatively low orbital variation seems to escape elucidation. However, our analysis detects a feature at termination V which makes it unique. The fact that termination V is the most prominent one is possibly the consequence of the longest time interval ever observed

between two terminations (Table 1). Because there was no termination trigger after termination VI for 128 kyr, Earth's climate system went deeply into a full glacial mode and therefore would have responded strongly to the occurrence of the insolation canon at termination V. Also interesting in this context is that the midpoint of termination V from various $\delta^{18}O$ records (Table 1) is indistinguishably close to OT. However, it has to be kept in mind that uncertainties arise when translating core depth to calendar age. For instance, Raymo [22] and Huybers and Wunsch [23] assign an uncertainty of 13.6 and 11 kyr to termination V in their stacked $\delta^{18}O$ records, respectively.

3.5. Leads and lags around a termination: Phase differences between NH and SH?

There is an ongoing debate whether the warming signal at a termination was synchronous in both NH and SH or whether one hemisphere was leading the other [24,25]. Although the insolation canon identified by our analysis encompasses both hemispheres, it originates in the SH as the increase in midsummer insolation at 65 °S occurs about 10 kyr prior to its NH counterpart. Hence, we would expect that around a termination changes of $\delta^{18}O$ or δD, proxies for local temperature, in Antarctic ice would precede those in Arctic ice. Unfortunately, direct comparison of Antarctic and Arctic climate records is difficult as uncertainties arise from translating core depth to calendar age and synchronizing NH and SH records to a uniform time scale. Nonetheless, the SH origin of the insolation canon suggests that, if there are phase differences between NH and SH warming around a termination, it would rather be a SH lead than a lag.

3.6. Possible feedback mechanisms

The mathematical analysis presented here is capable of identifying all seven Late Pleistocene glacial

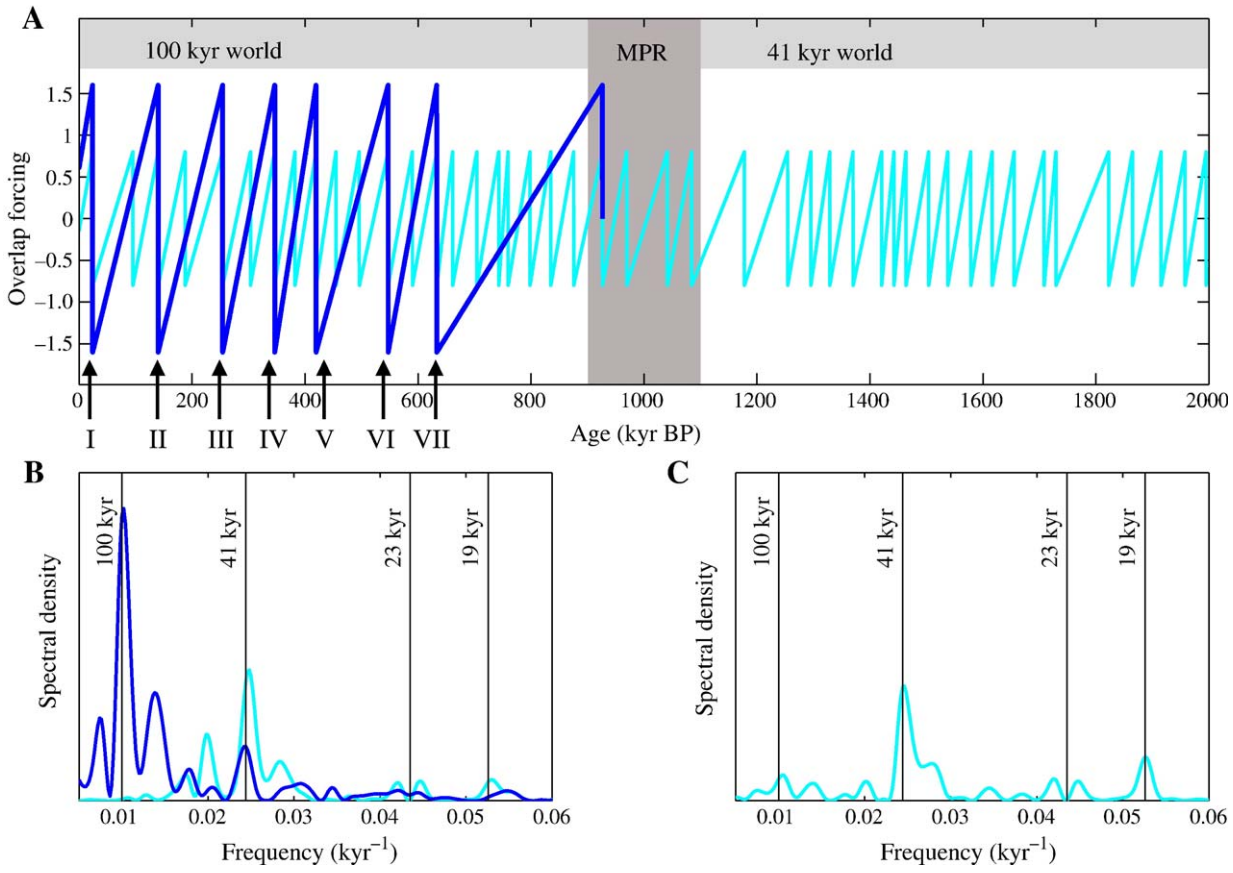

Fig. 7. Comparison of dominant frequencies predicted by the occurrence of overlaps in the Early and Late Pleistocene. (A) Sawtooth motifs through all overlaps in the Early and Late Pleistocene (light blue), and through the exceptional overlaps ('insolation canon'), excluding event A and B, in the Late Pleistocene (dark blue). Roman numbers denote respective terminations. (B) Power spectral densities against their frequencies of the oscillator through all overlaps (light blue) and through the prolonged overlaps, excluding event A and B (dark blue), in the Late and (C) Early Pleistocene.

terminations. It is free of interpretation or speculation regarding the response of Earth's climate system, which ultimately leads to deglaciation. However, the two thresholds of time and energy, fundamental to our termination trigger, suggest the involvement of particular feedback mechanisms. The necessity for a certain amount of energy supplied to the Antarctic and Arctic in the summer seasons indicates that sea-/land-ice melting, impacting deep water formation, are pivotal for these dramatic climate shifts. Although the responsible feedback between high latitude SH insolation forcing and the temporal SH lead during ice-age terminations has yet to be identified, the very feedbacks described above have been demonstrated operating during glacial terminations in the Antarctic [5,26,6]. These findings alone imply a dominant role of the SH during the initiation of deglaciation. However, according to our analysis, only the simultaneous increase in high latitude midsummer insolation in both hemispheres can push Earth's climate out of glacial conditions. We suggest that the tele-connection required is established by ocean circulation. The mixing time of this climate component, which holds the largest heat capacity and is responsible for bi-hemispheric heat transport, is about 1000 yr — just as our time threshold. The necessity for SH and NH synchrony may be found in the concept of the bipolar seesaw [27]. It has been observed that warming in the South leads to cooling in the North and vice versa [28,29]. Hence, a SH decrease in insolation always amplifies the NH warming forcing by insolation because SH and NH insolation changes are almost completely anti-phased. However, during the rare events of synchronous insolation increase (overlaps) both hemispheres would warm in parallel, triggered by this insolation canon. Thus, simultaneous warming could be pictured as repeated upward pushing at both ends of the seesaw, elevating its fulcrum point. This elevation might be thought to change temperature and ocean circulation. This would then ultimately set the stage for a variety of feedback mechanisms, e.g. reorganizations in the global carbon cycle (for a review see [30]), leading to the melting of the enormous '100 kyr' ice sheets in both hemispheres and thus for the transition to interglacial climate conditions.

3.7. The future

For the future, our analysis predicts the next termination trigger 53.4 kyr from now. However, model simulations predict an exceptionally long interglacial of 50 kyr ahead (see [31] and references therein) with the next glacial maximum and subsequent termination in 100 kyr. These models are highly sensitive to atmospheric CO_2, producing almost no NH glaciation with conditions above 290 ppmv. It is therefore questionable whether there will be any glaciation in the coming 100 kyr because atmospheric CO_2 is likely to stabilize around 400 ppmv 10 kyr from now [32] as a long-term result of fossil fuel burning by humans.

4. Summary and conclusions

Our analysis of changes in SH and NH midsummer insolation (65°) during the entire Pleistocene, the last 2 Myr, has revealed that prior to each Late Pleistocene glacial termination the insolation in both hemispheres increases in concert with a temporal SH lead. Such overlaps are not exclusively restricted to the occurrence of terminations. The overlaps at the seven Late Pleistocene glacial terminations, however, are exceptional as they are considerably longer and supply more energy compared to others. Overlaps are generated by variations in obliquity and precession and modulated by eccentricity. The concept of overlaps in general and of exceptional overlaps in particular (termed the 'insolation canon') could explain why 1) global ice volume in the Early Pleistocene is oscillating on a 41 kyr cyclicity, 2) in the Late Pleistocene an additional 100 kyr cyclicity appears, 3) Late Pleistocene glacial terminations occur at integer multiple of the precessional cycle, 4) the number of precessional cycles between each consecutive termination is not fixed (for example every fourth), and 5) the SH appears to play a pivotal role for the initiation of deglaciations. Therefore, we propose that the overlaps are involved in initiating global ice volume oscillations in the past, and that the insolation canon is the trigger of the Late Pleistocene glacial terminations.

Acknowledgments

We thank J. Laskar for generously providing us with the latest (1,1) astronomical solution of Earth's orbital parameters. We also thank him and J.M. Loutre for discussions regarding the contribution of each parameter to insolation. We acknowledge J. Bijma, W. Broecker, A. Körtzinger, G. Lohmann, L. Lourens, M. Maslin, G.-J. Raichart, M.E. Raymo, U. Riebesell and H. Spero for comments on the manuscript. We also thank P. Huybers for making available his EOFs.

References

[1] W.S. Broecker, J. Van Donk, The shape of climatic cycles as shown by the $\delta^{18}O$ record, Rev. Geophys. Space Phys. 8 (1970) 170–198.

[2] W.S. Broecker, Terminations, in: A.L. Berger, J. Imbrie, J. Hays, G. Kukla, B. Salzman (Eds.), Milankovitch and Climate, Part 2, D. Reidel Publishing Group, 1984, pp. 687–698.
[3] M. Milankovitch, Kanon der Erdbestrahlung und seine Anwendung auf das Eiszeitproblem, Vol. Spec. Publ. 132, 1941.
[4] A.J. Weaver, O.A. Saenko, P.U. Clark, J.X. Mitrovica, Meltwater Pulse 1A from Antarctica as a trigger of the Bølling–Allerød warm interval, Science 299 (2003) 1709–1713.
[5] G. Knorr, G. Lohmann, Southern Ocean origin for the resumption of Atlantic thermohaline circulation during deglaciation, Nature 424 (2003) 532–536.
[6] F.J.C. Peeters, R. Acheson, G.-J.A. Brummer, W.P.M. de Ruijter, R.R. Schneider, G.M. Ganssen, E. Ufkes, D. Kroon, Vigorous exchange between the Indian and Atlantic oceans at the end of the past five glacial periods, Nature 430 (2004) 661–665.
[7] A. Berger, Long-term variations of daily insolation and Quaternary climatic changes, J. Atmos. Sci. 35 (1978) 2362–2367.
[8] A. Berger, M.F. Loutre, Insolation values for the climate of the last 10 million years, Quat. Sci. Rev. 10 (1991) 297–317.
[9] J. Laskar, P. Robutel, F. Joutel, M. Gastineau, A. Correia, B. Levrard, A long term numerical solution for the insolation quantities of the earth, Astron. Astrophys. 428 (2004) 261–285.
[10] J. Imbrie, A. Berger, E.A. Boyle, S.C. Clemens, A. Duffy, W. Howard, G. Kukla, J. Kutzbach, D.G. Martinson, A. McIntyre, A.C. Mix, B. Molfino, J.J. Morley, L.C. Peterson, N.G. Pisias, W.L. Prell, M.E. Raymo, N.J. Shackelton, R. Toggweiler, On the structure and origin of major glaciation cycles 2. The 100,000-year cycle, Paleoceanography 8 (1993) 699–735.
[11] W.F. Ruddiman, Orbital insolation, ice volume, and greenhouse gases, Quat. Sci. Rev. 22 (2003) 1597–1629.
[12] M.A. Maslin, A. Ridgwell, Mid-Pleistocene Revolution and the 'eccentricity myth', Special Publication of the Geological Society of London 247 (2005) 19–34.
[13] D. Paillard, Glacial cycles: towards a new paradigm, Rev. Geophys. 39 (2001) 325–346.
[14] J. Laskar, F. Joutel, F. Boudin, Orbital, precessional, and insolation quantities from the Earth from −20 Myr to +10 Myr, Astron. Astrophys. 270 (1993) 522–533.
[15] H. Pälike, N.J. Shackleton, Constraints on astronomical parameters from the geologic record for the last 25 Myr, Earth Planet. Sci. Lett. 182 (2000) 1–14.
[16] L.J. Lourens, R. Wehausen, H. Brumsack, Geological constraints on tidal dissipation and dynamical ellipticity of the earth over the past three million years, Nature 409 (2001) 1029–1033.
[17] D. Paillard, The timing of Pleistocene glaciations from a simple multiple-state model, Nature 391 (1998) 378–381.
[18] D. Paillard, F. Parrenin, The Antarctic ice sheet and the triggering of deglaciations, Earth Planet. Sci. Lett. 227 (2004) 263–271.
[19] N.J. Shackelton, The 100,000-year ice-age cycle identified and found to lag temperature, carbon dioxide and orbital eccentricity, Science 289 (2000) 1897–1902.
[20] M.E. Raymo, K. Nisancioglu, The 41 kyr world: Milankovitch's other unsolved mystery, Paleoceanogr. 18 (1).
[21] A.J. Ridgwell, A.J. Watson, M.E. Raymo, Is the spectral signature of the 100 kyr glacial cycle consistent with a Milankovitch origin, Paleoceanography 14 (1999) 437–440.
[22] M.E. Raymo, The timing of major climate terminations, Paleoceanography 12 (1997) 577–585.
[23] P. Huybers, C. Wunsch, A depth-derived Pleistocene age model: Uncertainty estimates, sedimentation variability, and nonlinear climate change, Paleocenogr. 19 (1) (2004).
[24] T. Sowers, M. Bender, Climate records covering the last deglaciation, Science 269 (1995) 210–214.
[25] R.B. Alley, E.J. Brook, S. Anandakrishnan, A northern lead in the orbital band: north–south phasing of ice-age events, Quat. Sci. Rev. 21 (2002) 431–441.
[26] T.F. Stocker, South dials north, Nature 424 (2003) 496–499.
[27] W.S. Broecker, Paleocean circulation during the last deglaciation, Paleoceanography 13 (1998) 119–121.
[28] T. Blunier, E.J. Brook, Timing of millennial-scale climate change in Antarctica and Greenland during the last glacial period, Science 291 (2001) 109–112.
[29] J. Jouzel, R. Vaikmae, J.R. Petit, M. Martin, Y. Duclos, M. Stievenard, C. Lorius, M. Toots, Méliéres, L.H. Burckle, N.I. Barkov, V.M. Katiyakov, The two-step shape and timing of the last deglaciation in Antarctica, Clim. Dyn. 11 (1995) 151–161.
[30] M. Maslin, D. Seidov, J. Lowe, Synthesis of the Nature and Causes of Rapid Climate Transitions During the Quaternary, in: D. Seidov, B. Haupt, M.A. Maslin (Eds.), The oceans and rapid climate change: Past, present and future, AGU Geophysical Monograph Series, vol. 126, 2001, pp. 9–52.
[31] A. Berger, M. Loutre, An exceptionally long interglacial ahead? Science 297 (2002) 1287–1288.
[32] D. Archer, H. Kheshgi, E. Maier-Reimer, Dynamics of fossil fuel CO_2 neutralization by marine $CaCO_3$, Glob. Biochem. Cycles 12 (1998) 259–276.
[33] L.E. Lisiecki, M.E. Raymo, A Pliocene–Pleistocene stack of 57 globally distributed benthic $\delta^{18}O$ records, Paleoceanogr. 20 (2005).
[34] J. Imbrie, J.D. Hays, D. Martinson, A. McIntyre, A.C. Mix, J.J. Morley, N.G. Pisias, W.L. Prell, N.J. Shackleton, The orbital theory of Pleistocene climate: support from a revised chronology of the marine $\delta^{18}O$ record, in: A.L. Berger, J. Imbrie, J. Hays, G. Kukla, B. Salzman (Eds.), Milankovitch and Climate, Part 1, D. Reidel Publishing Group, 1984, pp. 269–305.